Rafidain Journal of Science
https://rsci.mosuljournals.com

Vol. 35, No. 1, pp. 82-93, 2026 (March)

Assessment of γ-AL_2O_3 Prepared from Local Clay as an Effective Catalyst for Thermal Cracking of Atmospheric Residue: Optimizations of Variables and Analysis of the Upgraded Liquid Oil

Ali A. Hussein **Abdelrahman B. Fadhil**

Department of Chemistry /College of Science/ University of Mosul

p-ISSN: 1608-9391
e -ISSN: 2664-2786

Article information

Received: 23/ 7/ 2025
Revised: 14/ 9/ 2025
Accepted: 24/ 9/ 2025

DOI: 10.33899/rsci.v35i1.61994

corresponding author:
Ali A. Hussein
aliammash8@gmail.com
Abdelrahman B. Fadhil
abdelrahmanbasil@uomosul.edu.iq

ABSTRACT

This research aims to synthesis of γ-Al_2O_3 catalyst from a local clay and studying the effect of calcination time and calcination temperature on the surface area of gamma alumina, to be employed as a catalyst in the thermal cracking of the atmospheric residue (ATR) taken from a local refinery in Mosul city, North of Iraq. The XRD, BET surface area and pore size, FESEM, and EDX for the resulting γ-Al_2O_3 were diagnosed. Using a 2.0 wt.% of γ-Al_2O_3 catalyst, the optimally upgraded liquid oil was produced at 400 °C for 1h, with an output of 79 % and a 40.55° API gravity. Fundamentally, the resulting liquid fuel was also analyzed using the resulting liquid fuel was also analyzed using Chromatography-Mass Spectrometry and H-NMR.

The results showed that the fuel consists of aromatics, n-alkanes, olefins, and iso-alkanes. Moreover, it’s gasoline content was 20 vol.%, with an octane-value of 82 In addition, the flash point and the kinematics viscosity of the resulting fuel were low. Eventually, the as-synthesized γ-Al_2O_3 could be recommended as a potential catalyst for the catalytic thermal cracking processes of heavy residue and oils.

Keywords: γ-Al_2O_3 catalyst, Atmospheric residue, Catalytic thermal cracking, Upgraded oil.

INTRODUCTION

Light crude oil supplies around the world have been decreasing as a result of rising demand for conventional oil due to rising populations and economies in recent years. Heavy oil, tar sand, and oil shale are some of the alternatives to conventional oil that have been necessary as a result of this (Topilnytskyy *et al.*, 2024; Yarmola *et al.,* 2023). Alkanes, cycloalkanes, aromatic compounds, and asphaltene—a heavy complex substance—are among the numerous hydrocarbons that make up petroleum products. The latter are separated into light, medium, heavy, and bitumen categories based on the American Petroleum Institute's (API) gravity (Thangaraj and Lee, 2024; Zhang *et al.*, 2020).

Heavy oil is difficult to handle and transport due to its heaviness, viscosity, and limited fluidity (Zhang *et al.*, 2020). Low-boiling-point hydrocarbon fractions vaporise without cracking during crude oil distillation at 350 °C at atmospheric pressure. The process produces gases, petrol, naphtha, diesel, kerosene, and atmospheric residue (ATR), which is formed in two separate columns during refining (Silv *et al.*, 2017). It has a high boiling point (>350 °C) and low API (~20°) depending on the crude oil used. Its asphaltene and resin composition give it a high boiling range and polarity (Hasan and Fadhil, 2023). This heavy fraction can also be used in thermal processes, like vacuum distillation to produce economically valuable distillates, as the atmospheric distillation may cause thermal cracking instead of distillation, reducing fractionation products (Hasan and Fadhil, 2023; Ali and Ali*,* 2021).

Gamma alumina has good mechanical properties, thermal stability, and a good surface area, which makes it an efficient catalyst in the thermal cracking process(Husein and Alkhaldi, 2014; Hussien and Mahmood, 2018; Al-Salman and Mohammad, 2006)

Thermal cracking, catalytic thermal cracking, coking, hydrocracking, solvent treatment, delayed coking, and visbreaking were used in transforming heavy distillates into high-quality products. ATR upgrades to more valuable products have been announced in literature. To obtain a high yield of light liquid, Kaminski and Husein (Kaminski and Husein, 2018) upgraded Arabian ATR in an autoclave at 400 °C for 1h. Hasan and Fadhil (Hasan and Fadhil, 2023) investigated thermal cracking Al-Dora ATR to make a fuel with a higher API gravity and lower viscosity. However, catalytic cracking is essential to petroleum refining. Heavy gas oil, vacuum distillation residue, and ATR are low-value oil fractions that it tries to turn into market-viable products. Zeolites, an alumina-silicate blend, are the main catalysts because of their acidic Bronsted or Lewis sites. (Silv *et al.*, 2017) studied the ATR catalytic thermal cracking over HY or HZSM-5 zeolites to recover more valuable liquid fuel. Nonetheless, alumina was commonly used as a catalyst or support for catalysts that turned heavy oils into lucrative distillates. (Esgair, 2016) used fluidised catalytic cracking to enhance Al-Duara ATR liquid oil. (Marafi *et al.*, 2006) tested MoO_3/Al_2O_3 as a demineralisation catalyst for Kuwaiti ATR and $Ni/MoO_3/Al_2O_3$ as a desulfurization catalyst for residence at 360-420 °C. As far as we know, synthesis of γ-Al_2O_3 from locally available rocks, to be tested as a catalyst in the thermal cracking of the ATR taken from Al-Kasik refinery, north of Iraq, to produce a high-grade synthetic liquid fuel (SLF) rich in light hydrocarbon fractions, like petrol and diesel fuel, have not been announced yet. This issue prompted us to examine and address this gap.

In this context, γ-Al_2O_3 was synthesised from local rocks and tried as a catalyst for the thermal cracking of ATR from Al-Kasik refinery, north of Iraq, to generate an improved SLF rich in gasoline and diesel hydrocarbons. Synthesis of the catalysts was optimized. The fuel characteristics, gasoline content, and octane number of the resulting gasoline were specified, as well. Also, the ^1H NMR and GC-MS spectroscopy were implemented to analyze the resulting SLF.

MATERIALS AND METHODS

1- Precursors and chemicals

The current study made use of ATR, which was generously supplied by the Al-Kasik refinery in northern Iraq, and kaolin clay, sourced from the Anbar Governorate in western Iraq, for the γ-

Al_2O_3 synthesis. Chemicals implemented here, including sulfuric acid (H_2SO_4 98%) and Abs. ethanol 99.99% were supplied from Scharlau chemicals, Spain.

2- Synthesis of γ-Al_2O_3

The kaolin clay was used to synthesize the support (γ-Al_2O_3). The kaolin was first pulverized with a powerful electric grinder, and then sieved through a 100-mesh screen. The kaolin powder was calcined in a muffle furnace to 800 °C for 2h. Afterwards, the calcined kaolin was treated with 2N of sulfuric acid at 1:20 ratio with the kaolin powder. A magnetic stirrer was used to continuously agitate the liquid as it was heated for 18 h. After letting the mixture cool to room temperature, it was filtered. In order to precipitate aluminium sulphate, the filtrate was removed and put in a burette. It was then gradually added to a flask that contained ethanol, which serves as a precipitating agent, while being constantly stirred. After being cleaned with ethanol once more and then distilled water, the latter was dehydrated for ten minutes at 70°C. The dried precipitate was then calcined for at various temperatures (600-900 °C) for numerous periods (1-4 h) (Hosseini *et al.*, 2011).

3- Characterization of γ-Al_2O_3 catalyst

Using an automated adsorption device (Micromeritics Tristar 3000), the surface area (BET) and pore volume of the γ-Al_2O_3 catalyst at 77 K were calculated by taking advantage of the N_2 adsorption–desorption. The γ-Al_2O_3 catalyst was degassed in a vacuum for three hours at 200°C before the measurement. To determine the crystalline structure of the as-synthesised γ-Al_2O_3 , a powder X-ray diffraction (XRD) examination was performed using an X' Pert Pro automatic powder diffractometer using Cu Kα (λ=0.15406 nm) 40 kV and 30 mA in the 2θ range of 10° to 90°. The JCPDS file database was used to identify the resulting peaks. The γ-Al_2O_3 surface morphology and elemental composition were obtained using a field emission scanning electron microscope (Tescan Mira 3 LMU FESEM-EDX, France, 2018) connected to an energy-dispersive X-ray analyser (EDX) at an emission voltage of 10 eV and an acceleration voltage of 20 kV.

4- Catalytic thermal cracking of the ATR

A cylindrical stainless-steel reactor surrounded by an electrical furnace was used in both catalytic and non-catalytic thermal cracking of ATR. Along with a temperature sensor, a carrier gas system, a condenser to liquefy the condensable liquid distillate, and a collector to gather the resultant liquid. A predetermined amount of ATR (25 mL) was added to the reactor in order to perform the thermal cracking tests. The necessary amount of γ-Al_2O_3 catalyst mixed with the ATR and mixed.

After that, the reactor was heated from room temperature until reaching the temperature needed for thermal cracking under a flow of N_2 gas. By investigating the effects of the catalyst amount (0.50-2.50 wt.%), the thermal cracking temperature (375-500 °C) with a 25 °C increments, and the thermal cracking time (1-2h) with increments of 30 min, the thermal cracking conditions of the ATR were optimized. Results from each run were recorded as the average ±SD after at least two runs. To determine how each variable affected the thermal cracking product yield, other variables were kept constant when optimizing other variable. The yield of the SLF produced was calculated, as follows (Ibrahim and Fadhil, 2023).

$$\text{Liquid yield (\%)} = \frac{\text{Volume of the produced SLF (mL)}}{\text{Volume of the ATR uitlized (mL)}} \text{ X } 100$$

5- Analysis and liquid fuel

The generated SLF was analyzed using ^1H NMR spectroscopy, which was performed on a 400-MHz instrument manufactured by Bruker Biospin GmbH in Germany. The solvent used was $CDCl_3$, and Tetramethyl Silane (TMS) was used as the internal reference solution. Using a Shimadzu gas chromatography-mass spectrometer (GC-MS-QP2010S, Japan) with an Omega Wax TM 250 column (30 m length, 0.25 mm diameter, and 0.25 μm film thickness) in the presence of He as the carrier gas, types of chemicals forming the SLF, were quantified.

6- Fuel properties evaluation of liquid fuel

The fuel properties of the SLF were also determined, including the density at 15.6 °C (D), the gravity at the API, the kinematic viscosity at 40 °C (KV), the flash point (FP), the amount of petrol, and the octane number of the fuel. Measurements were taken in accordance with the standard test procedures established by the ASTM.

RESULTS AND DISCUSSION

Optimization of catalysts preparation

The γ-Al_2O_3 catalyst was synthesized employing an optimized approach to produce the most effective catalyst for superior catalytic performance in the thermal cracking of the ATR, as depicted in Fig. (1) The raw alumina was calcined at temperatures ranging from 600 °C to 900 °C for 3 h, to evaluate the influence of calcination temperature on the surface area of the resulting γ-Al_2O_3 catalyst.

Fig. (1a) illustrates that the surface area of the resulting γ-Al_2O_3 enhanced when the calcination temperature raised from 600 °C to 700 °C, suggesting that the latter is the best temperature to produce γ-Al_2O_3 with a well-developed porous structure .Whereas water molecules were removed at a temperature below 600, while temperatures above 700 were required to remove the gas SO_3. Nonetheless, temperatures beyond 700 °C caused a reduction in the surface area of the γ-Al_2O_3, may be due to the sintering of the γ-Al_2O_3 particles (Matori *et al.*, 2012; Wang *et al.*, 2008).

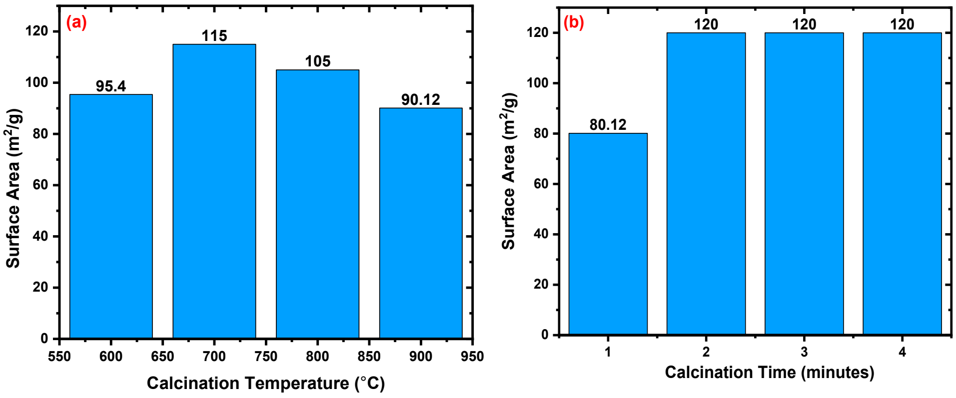

Fig. 1: (a) Effect of the calcination temperature on the surface area of the produced γ-Al_2O_3
(b) Effect of the calcination temperature on the surface area of the produced γ-Al_2O_3

Evaluating the impact of the calcination time of the resulting alumina, the latter was calcined at 700 °C for caried durations (1-4 H) at a heating rate of 10 °C/min. Data presented in Fig. 1(b) indicated that extending the calcination duration from 60 minutes to 120 minutes improved the surface area of the resulting γ-Al_2O_3, while periods above 2h no change in the surface area of the produced γ-Al_2O_3, (Wang *et al.*, 2011). Consequently, the γ-Al_2O_3 that was synthesized via calcinating the raw alumina at 700 °C for 2h at a 10 C/min rate of heating, will be tried as a catalyst in the catalytic thermal decomposition of the ATR.

Characterization of γ-Al2O3 catalyst

The typical γ-Al_2O_3 was further characterized to ascertain its crystalline structure, texture, and morphological attributes using various techniques. The N_2 adsorption-desorption isotherms of the as-synthesized γ-Al_2O_3 was refereed to type IV shape, as per the IUPAC classification, with the occurrence a hysteresis loop, indicating its mesoporous structure (Zaki *et al.*, 2013). The synthesised γ-Al_2O_3 exhibited a specific surface area (SA_{BET}) of 107.39 m^2/g and an average pore diameter of 27.50 nm, affirming its mesoporous structure. Fig.2.illustrate the N_2 adsorption-desorption isotherms and pore size distribution of the as-prepared γ-Al_2O_3.

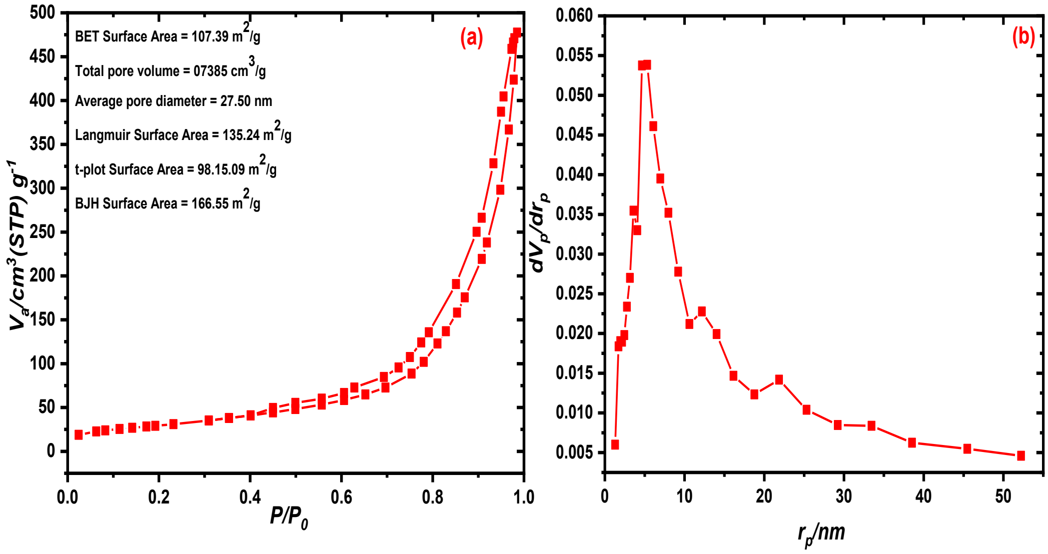

Fig. 2: N_2 adsorption-desorption isotherms and pore size distributionof as-synthesized ɤ-Al_2O_3 catalyst.

The crystalline structure of the resulting γ-Al_2O_3 was examined through the XRD analysis, which its diffractogram is demonstrated in Fig. (3). The XRD pattern indicated to the occurrence of four distinguishing peaks of γ-Al_2O_3 at different positions, as follows: 2θ= 20.1°; 2θ=37.15°; 2θ=47.85°; 2θ=67.10 °. Diffraction peaks that represent the α-Al_2O_3 could be detected at 2θ= 27.1° and 2θ= 57.2° (Mgbemere and Oluigbo, 2024). It is obvious from Fig. (3) that number of the diffraction peaks belonging to the γ-Al_2O_3 were greater than that representing α-Al_2O_3. Also, the diffractions peaks for γ-Al_2O_3 were broader than those belong to α-Al_2O_3, indicating that the percentage of γ-Al_2O_3 in the as-created alumina was above that represents α-Al_2O_3.

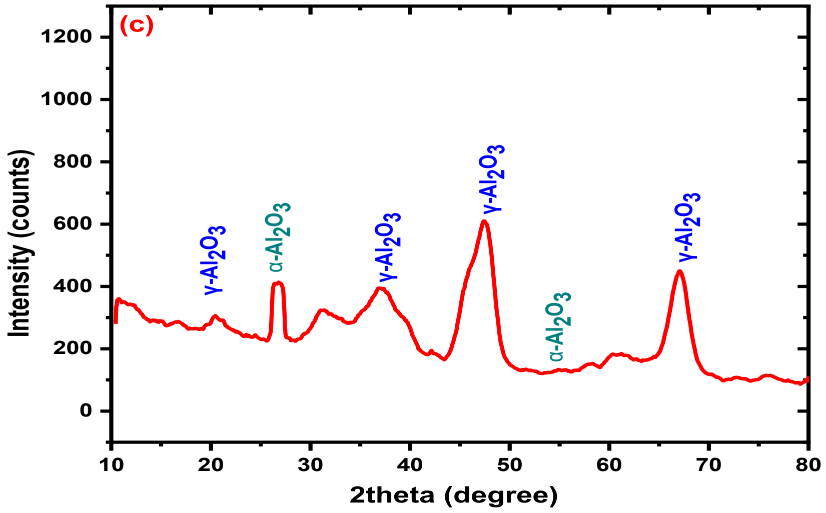

Fig. 3: XRD patterns of as-synthesized ɤ-Al_2O_3 catalyst.

The EDX technique was used to analyze the elemental composition of the resultant γ-Al_2O_3. The EDX mapping of γ-Al_2O_3 Fig. (4) revealed that Al (42.76%) and O (57.24%) were the primary elements, indicating the purity of the as-created γ-Al_2O_3.

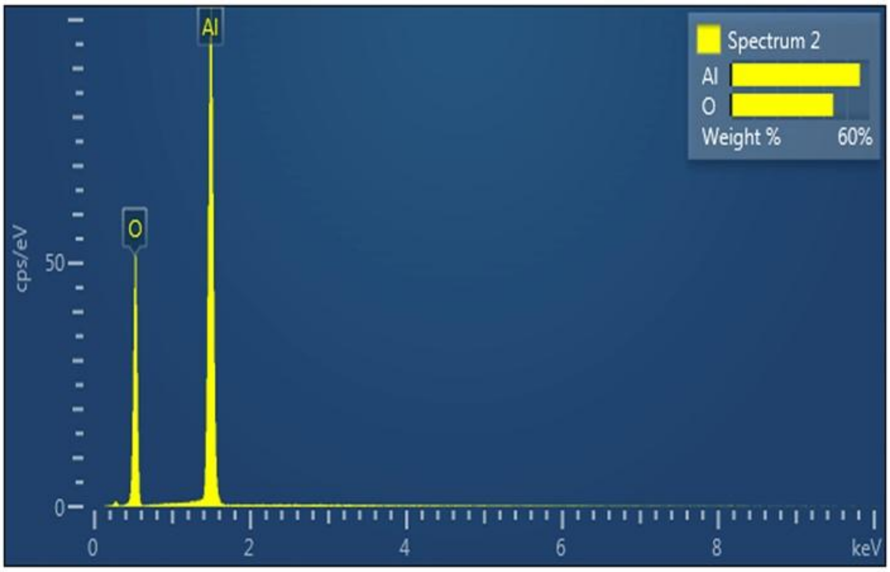

Fig. 4 :EDX mapping of as-synthesized ɤ-Al_2O_3 catalyst.

Fig. (5) shows FESEM images of as-created γ-Al_2O_3 at multiple magnifications. The FESEM images revealed that, although some clusters with irregular shapes could be observed on its surface, the resulting γ-Al_2O_3 exhibited an amorphous surface, due to the existence of many cracks and voids with different shapes and sizes. These findings match the SA_{BET} measurement, which was high and confirmed its amorphous nature of the prepared γ-Al_2O_3.

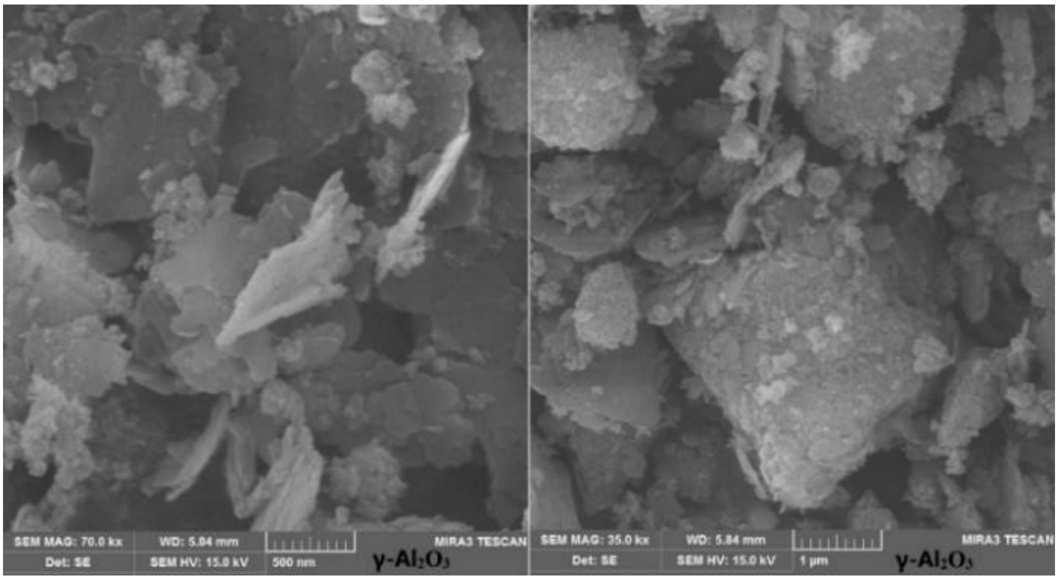

Fig. 5: FESEM images of as-synthesized ɤ-Al_2O_3 catalyst.

Catalytic thermal cracking of ATR by γ-Al2O3 catalyst

The incorporation of a catalyst enhances the characteristics and composition of the liquid fuel. Optimal catalyst amount is essential for maximising liquid fuel production due to its considerable influence (Soltanali *et al.*, 2020). The catalytic thermal cracking of the ATR was conducted at 450 °C adopting different quantities of the γ-Al_2O_3 catalyst, ranging from 0.50 wt.% to 3.0 wt.%.

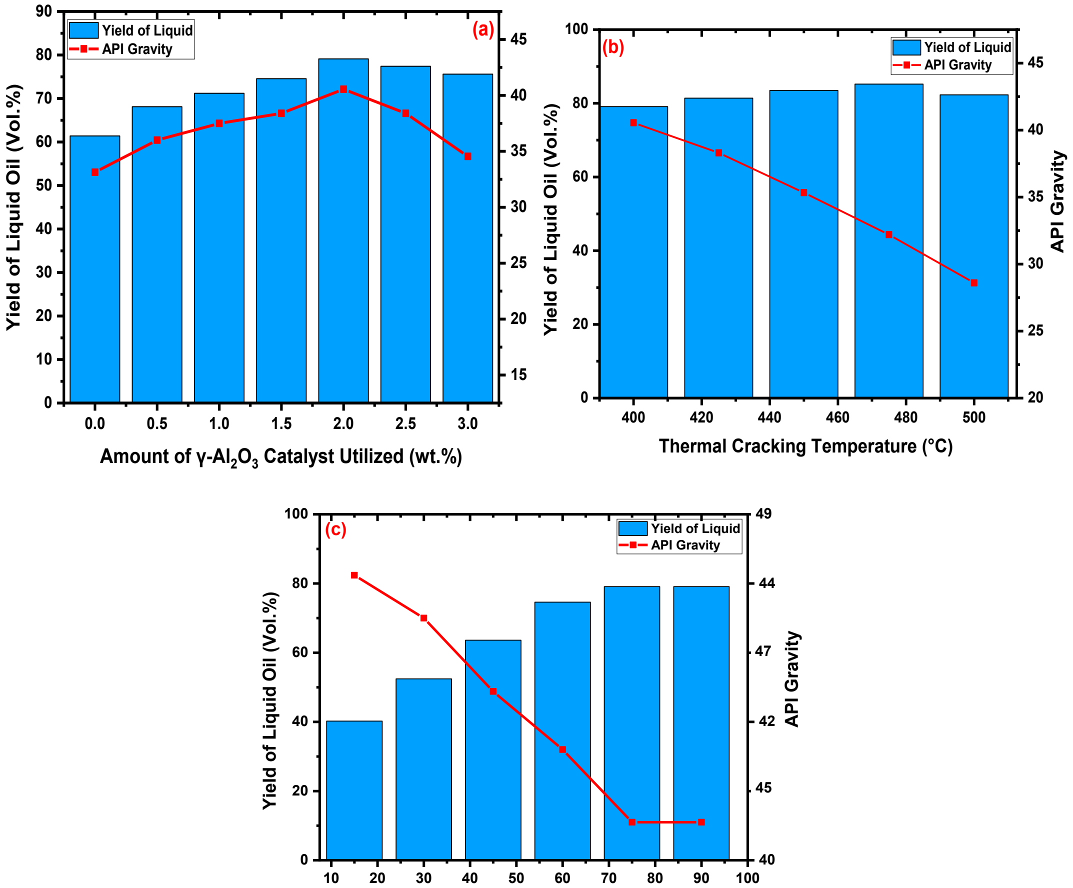

Fig. 6: The Effect of the thermal cracking conditions on the output and API gravity of the produced liquid oil.

Fig. (6-a) illustrates that the production of the liquid fuel increased from 61.0% (non-catalytic process) to 84.0 % for the thermal cracking of the ATR. In contrast to the non-catalytic thermal cracking process, the introduction of the γ-Al_2O_3 catalyst significantly enhanced the liquid fuel yield by promoting synergistic interactions between ATR and the catalyst's active regions, leading to greater liquid fuel production(Ibrahim and Fadhil, 2023; Aljeradat *et al*., 2022). The increase in liquid fuel yield with the addition of catalyst in the thermal cracking of ATR is attributed to the rise in the number of catalytically active sites that enhance the process, resulting in superior liquid output (Ibrahim and Fadhil, 2023). It is believed that the introduction of a catalyst was announced to enhance liquid output through two mechanisms: surface and pore reactions. The catalyst surface reaction transpires with a reduced catalyst dosage, whereas an increase in catalyst loading results in pore reaction (Ibrahim and Fadhil, 2023; Aljeradat *et al*., 2022). Nonetheless, beyond the appropriate dosage of the catalyst correlated with a reduction in the yield of the liquid fuel. Increasing the quantity of the catalyst augmented the number of catalytically active sites, hence enhancing the secondary cracking of the initial ATR into non-condensable components. As a result, the production of liquid fuel decreases (Ibrahim and Fadhil, 2023; Aljeradat *et al*., 2022).

The API gravity was employed as an indicator of the quality of the produced fuel. Fig. (6-a) clearly indicates that the presence of the catalyst increased the API gravity of the resultant liquid fuel in comparison to the original ATR. Furthermore, an increase in the catalyst quantity utilised in the thermal cracking process enhanced the API gravity of the resultant liquid. These results indicate that the catalyst will commence thermal cracking of the unaltered ATR into smaller molecular weight products, yielding a liquid sample with improved API gravity. The maximum API gravity was recorded with the liquid fuel generated employing 2.0 wt.% of the catalyst, whereas an increased catalyst quantity diminished the API gravity of the resulting liquid. This conclusion results from utilising a greater quantity of the catalyst, which triggers the thermal breaking of the heavier components of the ATR, yielding a liquid fuel with less API gravity.

Using 2.5 wt.% of the as-synthesized γ-Al_2O_3 catalyst, many temperatures (400-500 °C) with a 25 °C increments per test were tried during the ATR catalytic thermal pyrolysis. Because of the incomplete thermal breakdown of the authentic ATR, the liquid fuel's output was minimal at lower temperatures. With the progress of the pyrolysis temperature, the liquid output grew as well.

Nonetheless, the liquid production beyond 500 °C decreased, as shown in Fig. (6-b). It was noticed that a temperature of 475 °C produced the maximum liquid's output. The increment of the liquid oil yield with expanding thermal decomposition temperature suggests the rapid endothermic degradation of the ATR, and also indicates to further decomposition of the heavier fractions of the ATR, leading to a higher output of the liquid oil. Temperatures exceeding 475 °C decreased the production of liquid oil, perhaps because of thermal cracking of the pristine ATR or condensable volatiles into non-condensable vapors, causing a drop in the output of the produced oil. When the temperature of thermal cracking of the pristine ATR raised from 375 °C to 400 °C, the produced liquid oil had exhibited the highest API gravity. However, with further progress in thermal cracking temperature, a decline in the API gravity for the resulting samples occurred, may be due to that conducting thermal pyrolysis of the feed at higher temperatures in the occurrence of sufficient amount of catalyst will aid in the decomposition of the heavier components of the real ATR, producing heavier liquid oil, and consequently, API gravity of the resulting oil diminished.

The duration that the feed must spend inside the reactor, which affects the output of liquid oil, is another important aspect that must be controlled during the thermal destruction process of the ATR, as the duration of contact between the feed and the heating region is controlled by this variable (Ibrahim and Fadhil, 2023). Accordingly, the best time for the process should be carefully chosen.

So, as shown in Fig. (6-c), the catalytic pyrolysis of the ATR was carried out at various periods within the range of 15 to 90 minutes, while keeping all other variables unchanged. Because there was insufficient heat transfer from the pyrolysis zone to the feed through conduction, the ATR was not completely broken down into the required products, as this figure illustrates, and the brief pyrolysis durations did not create the maximum output of the liquid fuel (Ibrahim and Abdelrahman., 2023).

The output of liquid oil increased when the pyrolysis period stretched from 15 to 75 minutes, whereas it dropped when it was extended beyond 75 minutes. While longer time periods did not give any change in the outcome due to the end of the reaction. (Ibrahim and Fadhil, 2023). The API gravity of the resulting liquid oil decreased as the thermal decomposition time increased Fig. (6-c). This is because, in the presence of the catalyst, the original ATR will further break down into heavier fractions with extending the thermal cracking period, and thereby lowering the API gravity.

Additionally, there is a chance for the generated oil to be further break down into non-condensable gases with prolonging the pyrolysis time, leaving behind a heavier liquid with a greater API gravity.

Analysis of the liquid oil

The liquid oil produced under the ideal conditions of the catalytic thermal cracking process of the ATR (400 °C; 1.15h; 2.0 wt. % of γ-Al2O3) was analyzed using a number of instruments, including ^1H NMR spectroscopy, to ascertain its chemical composition. According to the ^1H NMR findings, (Table.1) and Fig. (7) show the majority of hydrogens in resulting oil were aliphatic with a ratio of 73.21 %. On the other hand, the aromatic-H amounted to 13.91 %. The olefinic-H could also be detected in the resulting oil fraction, which are thought to exist because the thermal cracking of the native ATR. Also, there presence assures that the authentic ATR was thermally cracked. At the same time, the oil fraction produced under the catalytic thermal cracking settings the resulting oil was also primarily composed of aliphatic hydrogen, constituting 92.68% compared with 7.32 % for the aromatic H. On top of that, the aliphatic-H made up the majority of the oil fraction generated under the catalytic thermal cracking conditions, accounting for 92.68 % of the total, as opposed to 7.32 % for aromatic-H. Furthermore, the resultant oil lacked the olefinic -H, which might be hydrogenated by the H_2 gas produced during the pyrolysis process or/and they were further dehydrogenate into straight hydrocarbons.

Table 1: Percentages and chemical shift of hydrogen distribution of the liquid oils.

Parameter	Chemical shift (ppm)	Definition	Value	
			Liquid oil 1	Liquid oil 2
HA	6.5-9.0	Aromatic protons	13.91	7.32
Hal	0.50 – 4.50	Total aliphatique hydrogène	73.21	92.68
Hol	4.5-6.5	H attached to oléfinique Carbon	6.45	0
Hal:α	1.9-4.5	Aliphatic H in α–position to aromatic ring	59.38	26.24
Hal:β	1.0-1.90	aliphatic H in β–position to aromatic ring	0.0	38.17
Hal: γ	1.0-0.5	Aliphatic H in γ–position to aromatic ring	16.87	28.24
[1]Liquid oil produced via non-catalytic process ; [2]Liquid oil produced via catalytic process				

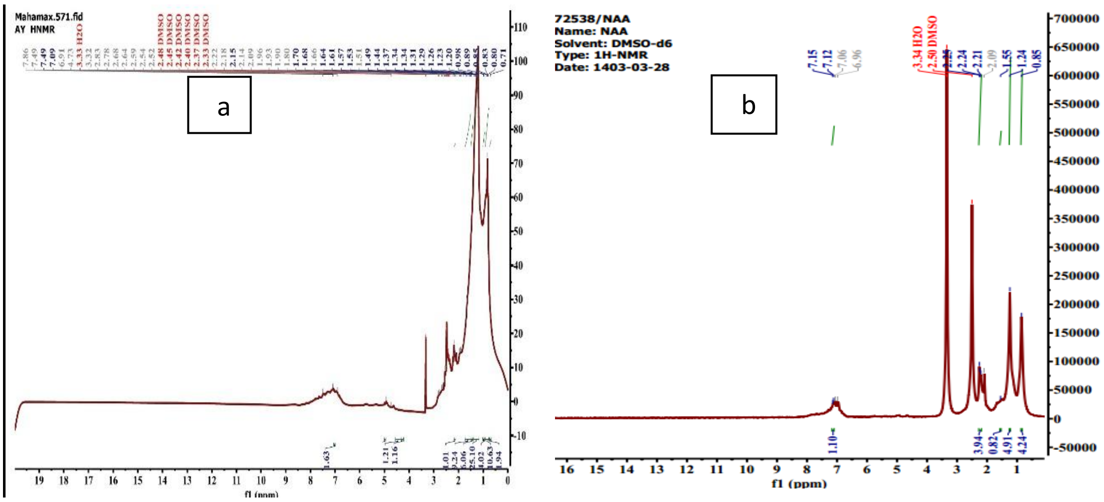

Fig. 7: (a) chart of H NMR for liquid produced without catalyst, and (b) chart of H NMR for liquid produced using Al_2O_3 catalyst

To determine the chemical components that forming the resultant oil produced with and without the catalyst, GC-MS spectroscopy was implemented. According to the findings deduced from the GC-MS analysis, which are depicted in Fig. (8). the liquid fraction that is generated as a result of the non-catalytic thermal degradation of the ATR is mostly composed of n-alkanes (62.17%), aromatics (12.70 %), iso-alkanes (6.22 %), alkenes (8.04%), and naphthenes (3.82%). The liquid fraction produced by the non-catalytic thermal degradation of the ATR was primarily composed of n-alkanes (62.17%), aromatics (12.70%), iso-alkanes (6.22%), alkenes (8.04%), and naphthenes (3.82%), as deduced from the GC-MS analysis, which its outcomes are shown in Fig. 4. Conversely, the oil fraction created via the catalytic thermal degradation of the ATR, was chiefly composed of naphthenes (2.1%), alkenes (2.05%), iso-alkanes (10.55%), aromatics (15.6%), and n-alkanes (58.2%). The catalytic thermal cracking of the ATR resulted in a lower concentration of n-alkanes in the liquid fuel compared to the non-catalytic process, as can be shown in Fig. (4). The finding might be because of the isomerization reactions that transform n-alkanes into iso-alkanes. However, the aromatics content in the liquid oil produced through the catalytic thermal cracking of the ATR was greater than that in the resulting oil from the non-catalytic process. One possible explanation for these findings is that the dehydrogenation processes are transforming n-alkanes or olefines into aromatics.

Fig. (8). also shows that compared to the catalytic approach, the non-catalytic process resulted in a substantially larger percentage of naphthenes in the liquid oil than that produced by the catalytic approach. Such findings could be ascribed to the existence of the catalyst, which speeds up the dehydrogenation processes of naphthenes into aromatics. Similarly, the content of olefines. As a consequence, it can be concluded that including γ-Al_2O_3 as catalyst during the thermal breakdown of the original ATR led to a superior upgraded oil compared to the non-catalytic approach.

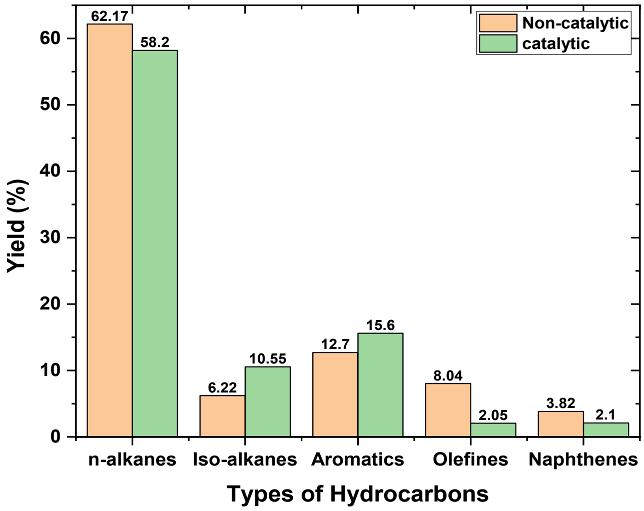

Fig. 8: Types of hydrocarbons form the produced liquid oils.

Fuel properties evaluation

Evaluation of the fuel characteristics, gasoline content, and octane number of the liquid oils obtained from the catalytic thermal cracking of the ATR were adopted and compared with those of the original ATR besides the liquid fuel produced through the non-catalytic thermal cracking process of the same ATR, under the ideal working settings. According to (Table 2), the fuel qualities of the liquid oil synthesized through the catalytic thermal cracking approach of the ATR were superior to those of the actual ATR and much better than those of the liquid oil produced by the non-catalytic thermal cracking method. Such finding might be ascribed to the occurrence of the catalyst (γ-Al_2O_3), which changes mechanism of the thermal cracking process, resulting in a more advanced fuel with better fuel properties and a higher petrol content than the non-catalytic process. In consequence, employing γ-Al_2O_3 as a catalyst on the thermal decomposition led to create a high-quality synthetic oil having characteristics comparable to traditional crude oils. Consequently, this synthetic fuel can be recommended as a liquid feedstock for classical refineries. Additionally, the increased concentration of iso-alkanes and aromatics in gasoline separated from from liquid oil produced by the catalytic thermal cracking technique results in a higher octane-number compared to petrol produced via the non-catalytic process.

Table 2: Fuel properties of the distillate liquid fuels.

Property	ATR	Liquid Fraction	
		Liquid Fraction a	Liquid Fraction b
Specific Gravity@ 15.60 °C	0.9473	0.85	0.8224
API Gravity	16.68	34.26	40.55
Kinematic Viscosity@ 40 °C	160.0	4.7	2.4
Flash Point, °C	130.0	67	Flammable
Asphaltenes %	16.50	0.32	0.10
Maltenes %	83.50	99.68	99.90
Gasoline content (v %)	-	15	20
RON	-	80	82

CONCLUTIONS

The as-synthesized γ-Al_2O_3 catalyst shown a promising performance in the ATR thermal cracking process. It led to the creation of a synthetic fuel with an output of 79 % and an API gravity of 40.55 at 400 C° and 75 minutes, compared to the liquid fuel synthesized without a catalyst, which had an output of 61.4% and an API gravity of 34.26 at 400 C° and 90 minutes. Also, gasoline fuel separated from liquid oil produced by the catalytic process had an octane number of 82.0, compared with 80.0 for that crated by the non-catalytic process, and the cause belongs to the elevated levels of aromatics and iso-alkanes in the former relative to the latter. In conclusion, the γ-Al_2O_3 catalyst developed here in is recommended as a viable catalyst for the catalytic thermal cracking of heavy oils, heavy distillates and oil residue.

ACKNOWLEDGMENT

The authors express gratitude to the University of Mosul, College of Science, Chemistry Department, for supporting of this research.

REFERENCES

Al-Salman, Y. A.; Mohammad, M. A. (2006). Using of nickel oxide nio as a diffusion barrier in aluminide coating on austinitic stainless steel aisi 321. *Raf. J. Sci.*, **17**(6), 22-32.

Ali, N. M.; Naife, T. M. (2021). Deasphalting of atmospheric Iraqi residue using different solvents. *J. Eng.*, **27**(5), 17-27. DOI: 10.31026/J.ENG.2021.05.02.

Aljeradat, R. A.; Aljbour, S. H.; Jarrah, N. A. (2022). Pyrolysis of date kernels using natural Jordanian tripoli as a catalyst under different operational conditions. *Case Stud. Chem. Environ. Eng.*, **6**, 100212. DOI: 10.1016/J.CSCEE.2022.100212.

Esgair, K. K. (2016). The catalytic activity of modified zeolite lanthanum on the catalytic cracking of al-duara atmospheric distillation residue. *J. Eng.*, **22**(3), 36-48. DOI: 10.31026/J.ENG.2016.03.03.

Hasan, R. A.; Fadhil, A. B. (2023). Conversion of atmospheric residue into upgraded fuel and carbon adsorbent for the adsorptive desulfurization process. *Fuller. Nanotub. Car. N.*, **31**(5), 423-434. DOI:10.1080/1536383X.2023.2169676.

Hosseini, S. A.; Niaei, A.; Salari, D. (2011). Production of γ-Al2O3 from Kaolin. *Open J. Phys. Chem.*, **1**(2), 23-27. DOI:10.4236/OJPC.2011.12004.

Husein, M. M.; Alkhaldi, S. J. (2014). In situ preparation of alumina nanoparticles in heavy oil and their thermal cracking performance. *Ene. Fue.*, **28**(10), 6563-6569. DOI:10.1021/EF5012963.

Hussien, A. K.; Mahmood, A. D. F. (2018). Effect of fillers on the adhesion properties of the cured unsaturated polyester adhesive. *Raf. J. Sci.*, **27**, 65-72.

Ibrahim, A. S.; Fadhil, A. B. (2023). Pyrolysis of date stones using natural activated kaolin as a catalyst–optimization of variables and identification of bio-oil. *J. Ecol. Eng.*, **24**(10). DOI:10.12911/22998993/170276.

Kaminski, T.; Husein, M. M. (2018). Thermal cracking of atmospheric residue versus vacuum residue. *Fuel Process. Technol.*, **181**, 331-339. DOI: 10.1016/j.fuproc.2018.10.014.

Marafi, A.; Hauser, A.; Stanislaus, A. (2006). Atmospheric residue desulfurization process for residual oil upgrading: An investigation of the effect of catalyst type and operating severity on product oil quality. *Ene. Fue.*, **20**(3), 1145-1149. DOI:10.1021/EF050395D.

Matori, K. A.; Wah, L. C.; Hashim, M.; Ismail, I.; Zaid, M. H. M. (2012). Phase transformations of α-alumina made from waste aluminum via a precipitation technique. *Int. J. Mol. Sci.*, **13**(12), 16812-16821. DOI:10.3390/IJMS131216812.

Mgbemere, H.; Oluigbo, C. (2024). Synthesis of alumina from kaolin found in Ajebo, Ogun state, Nigeria. *Eskisehir Tech. Univ. J. Sci. Technol. A - Appl. Sci. Eng.*, **25**(1), 115-122. DOI:10.18038/ESTUBTDA.1375497.

Silva, J. B.; Oliveira, J. M.; Almeida, L. S. (2017). Catalytic distillation of an atmospheric petroleum resid using HZSM-5 and HY zeolites. *Pet. Sci. Technol.*, **35**(19), 1938-1943. DOI:10.1080/10916466.2017.1373127.

Soltanali, S.; Mashayekhi, M.; Mohaddecy, S. R. S. (2020). Comprehensive investigation of the effect of adding phosphorus and/or boron to NiMo/γ-Al2O3 catalyst in diesel fuel hydrotreating. *Pro. Saf. Environ. Prot.*, **137**, 273-281. DOI: 10.1016/J.PSEP.2020.02.033.

Thangaraj, B.; Lee, Y. K. (2024). Recent progress in catalytic aquathermolysis of heavy oils. *Fuel*, **372**, 132089. DOI:10.23939/CHCHT18.02.258.

Topilnytskyy, P.; Shyshchak, O.; Tkachuk, V.; Palianytsia, L.; Chupashko, O. (2024). Advanced research on the production, transportation and processing of high waxy oil. A review. *Chem. Chem. Technol.*, **18**(2), 258-269. DOI:10.23939/CHCHT18.02.258.

Wang, S.; Li, X.; Wang, S.; Li, Y.; Zhai, Y. (2008). Synthesis of γ-alumina via precipitation in ethanol. *Mater. Lett.*, **62**(20), 3552-3554. DOI: 10.1016/J.MATLET.2008.03.048.

Wang, X. Y.; Wang, H. J.; Hou, G. Q.; Lv, Z. X. (2011). Preparation of activated alumina admixture. *Appl. Mech. Mater.*, **84**, 489-493. DOI: 10.4028/WWW.SCIENTIFIC.NET/AMM.84-85.489.

Yarmola, T.; Topilnytskyy, P.; Romanchuk, V. (2023). High-Viscosity Crude Oil. A Review. *Chem. Chem. Technol.*, **17**(1), 195–202. DOI:10.23939/CHCHT17.01.195.

Zaki, T.; Mohamed, N. H.; Nessim, M. I.; Abd El Salam, H. (2013). Characterization and application of nano-alumina sorbents for desulfurization and dearomatization of Suez crude petrolatum. *Fuel Pro. Technol.*, **106**, 625-630. DOI: 10.1016/J.FUPROC.2012.09.055.

Zhang, J.; Gao, H.; Xue, Q. (2020). Potential applications of microbial enhanced oil recovery to heavy oil. *Crit. Rev. Bio. techno.*, **40**(4), 459-474. DOI:10.1080/07388551.2020.1739618.

تقييم γ-AL2O3 المحضرة من الطين المحلي كمحفز فعال للتكسير الحراري لمخلفات التقطير الجوي: دراسة المتغيرات وتحليل الوقود السائل المُحسّن

علي عماش حسين **عبد الرحمن باسل فاضل**

قسم الكيمياء/ كلية العلوم/ جامعة الموصل/ الموصل/ العراق

الملخص

يتناول هذا البحث تحضير محفز γ-Al2O3 من طين محلي، ودراسة تأثير كل من زمن الكلسنة ودرجة حرارة الكلسنة للمساحة السطحية للكاما الومينا لاستخدامها كمحفز في التكسير الحراري للمخلفات الجوية (ATR) المأخوذة من مصفاة محلية في مدينة الموصل، شمال العراق. شخصت الكاما الالومينا المحضرة باستخدام طيف حيود الاشعة السينية والمساحة السطحية الكلية وحجم المسام اضافة الى صور المجهر الالكتروني والتحليل العنصري للعناصر. باستخدام كمية من حفاز الكاما الومينا 2% وزنا وتحت درجة حرارة 400 درجة مئوية وبزمن ساعة وربع تم الحصول على الوقود المثالي لهذه الدراسة بحصيلة بلغت 79% وقيمة دالة ال API كانت 40.55. اجريت فحوصات وباستخدام تقنية طيف الرنين النووي المغناطيسي وكروماتوغرافيا الغاز كتلة للوقود السائل الناتج حيث اظهرت الفحوصات ان الوقود الناتج يتكون مركبات اروماتية والالكانات خطية ومتفرعة اضافة الى مركبات اوليفينية. علاوة على ذلك بلغت نسبة محتوى الكازولين في الوقود السائل الذي تم إنتاجه 20% وقيمة الرقم الاوكتاني وصلت الى 82% اضافة الى ذلك ان قيمة درجة الوميض والزوجة للوقود الناتج كانت منخفضة. في الختام يمكن التوصية بان حفاز الكاما الومينا الذي تم تحضيره يمكن ان يستخدم كحفاز كفوء في عملية التكسير الحراري المحفز للمستقطرات النفطية الثقيلة.

الكلمات الدالة: الكاما الومينا، مخلفات التقطير الجوي، التكسير الحراري المحفز، تحسين النفط.